

TWO-DIMENSIONAL LOESS LANDSLIDE DEFORMATION MONITORING WITH MULTIDIMENSIONAL SMALL BASELINE SUBSET (MSBAS) -A CASE STUDY OF XINYUAN No.2 LANDSLIDE, GANSU, CHINA

C. Y. Zhao^{1,2,3*}, X. J. Liu¹, W. Zhu¹, W. F. Zhu¹

¹ School of Geology Engineering and Geomatics, Chang'an University, Xi'an 710054, China; zhaochaoying@163.com (C.Z.);
Xiaojie_Liu_cd@163.com(X. L.); zhuwu@chd.edu.cn (W. Z.); wenfeng_zhu@163.com (W. Z.)

²State Key Laboratory of Geo-Information Engineering, Xi'an, 710054, China

³National administration of surveying, mapping and geo-information, Engineering research center of national geographic conditions monitoring, Xi'an, 710054, China

Commission III, WG III/3

KEY WORDS: Landslide monitoring, InSAR, MSBAS, TerraSAR-X, Retrogressive failure

ABSTRACT:

The deformation monitoring of active landslides is of great importance for the safety of human lives and properties. And two-dimensional deformation result can give us more thoughts on the landslide type and deformation process. In this study, multidimensional small baseline subsets (MSBAS) technique is introduced and tested to compute two-dimensional deformation rate and time series for both east-west and vertical deformation of Xinyuan No.2 landslide by simultaneously processing ascending and descending TerraSAR-X data acquired from January 2016 to November 2016. Results show not only the spatiotemporal characteristics of this landslides, but the retrogressive loess landslide failure mode is revealed for the first time with the two-dimensional deformation.

1. INTRODUCTION

Loess occupies approximately 6.6% of the total area of China and exists in 12 provinces, of which 0.4 million square kilometers is loess plateau (Zhao et al., 2016). Loess plateau is an important base of energy sources and chemical industries in China, and it is also one of the regions with the most serious soil erosion and the most fragile ecological environment in the world. Loess plateau is prone to serious geo-hazard including collapse, landslide, earthflow, land subsidence and ground fissures (Qi et al., 2017), which seriously restrict the regional urban construction, economic development, and threaten the safety of transportation system and natural resource exploration. So, it is very important to identify in advance and monitor with high precision for these loess geo-hazards. Xinyuan No.2 landslide, located in the arid loess plateau, Gansu province, China is as small as 150m in length and 160m in width (Figure 1). People began to pump a large amount of water from the Yellow River for agricultural irrigation since the 1960s. Therefore, the long-term irrigation resulted in the groundwater level rising over 100cm in two years, the basal zone of loess is softened by saturation and readily to deform under overburden stress (Peng et al., 2017; Qi et al., 2017; Xu et al., 2011). As a result, a large number of loess landslides have occurred in this region (Figure 1) (Zhang et al., 2011).

In recent years, different InSAR technique have been widely used in landslide detection and monitoring (Zhao et al., 2012; Zhao et al., 2013; Zhao et al., 2016; Rosi et al., 2017). Usually, phase-based methods including differential SAR interferometry (D-InSAR), small baseline subset (SBAS), persistent scatterer InSAR (PSI) and their combination method are applied to measure landslide displacements in line-of-sight (LOS) direction. However, aiming to monitoring small scale and analyzing landslides mode, the following technical issues remain. It can only process one SAR dataset at once; it can only obtain one-dimensional LOS deformation; and the temporal resolution

defined by satellite revisit time is low. In what follows, two-dimensional deformation monitoring method is introduced and high temporal resolution results are obtained.

To overcome the disadvantages of traditional one-dimensional multi-temporal InSAR methods, advanced multidimensional small baseline subsets (MSBAS) technique is introduced, with which two-dimensional deformation rate and time series deformation in both east-west and vertical directions are calculated.

2. METHODOLOGY

The MSBAS technique combines multiple D-InSAR datasets into a single solution, which has two kinds of improvement in terms of noise decreasing and temporal resolution increasing with almost uninterrupted temporal coverage (Tiampo et al., 2017). The MSBAS methodology is an extension of the original SBAS method that reconstructs two or three-dimensional deformation rate and time series from ascending and descending InSAR data acquired by different SAR sensors considering various characteristics including wavelength, temporal and spatial resolution, azimuth and incidence angles (Samsonov et al., 2014). The precision of MSBAS-derived results are affected by the quality of interferograms and some processing parameters including phase filtering strength, coherence threshold for unwrapping, location of reference point, techniques for the removal of spatially and temporally correlated atmospheric noise and residual orbital trend.

If a single set of SAR data acquired by a sensor with an incidence angle θ and an azimuth α , the time series deformation can be reconstructed by applying the SBAS method (Berardino et al.,).

$$AV_{los} = \phi_{obs}, V_{los} = A^+ \phi_{obs}, d_{los}^{i+1} = d_{los}^i + V_{los}^{i+1} \Delta t^{i+1} \quad (1)$$

* Corresponding author

where A is an $M \times N$ matrix (M is the number of interferograms and $N+1$ is the number of SAR images), V_{los} is the LOS velocities, ϕ_{obs} is the observed phase. A^+ is a pseudo-inverse of matrix A calculated by Singular Value Decomposition (SVD), and d_{los}^i is the LOS displacement at the epoch t^i .

When K multiple SAR datasets are available with different incidence angles and azimuth, the Eq. (1) can be rewritten in the following form (Samsonov et al., 2013):

$$\begin{bmatrix} S_N^k A & S_E^k A & S_U^k A \end{bmatrix} \bullet \begin{bmatrix} V_N & V_E & V_U \end{bmatrix}^T = \phi_{obs}^k \quad (2)$$

$$V_{los} = SV = S_N V_N + S_E V_E + S_U V_U \quad (3)$$

where S is a unit vector of LOS with north, east and up components, and V is a velocity vector with components V_N , V_E , V_U .

The MSBAS method that includes all K sets of independently acquired SAR data can be expressed in the following equation:

$$\begin{pmatrix} A^1 \\ A^2 \\ \dots \\ A^K \end{pmatrix} \times \begin{pmatrix} V_N \\ V_E \\ V_U \end{pmatrix} = \begin{pmatrix} \phi^1 \\ \phi^2 \\ \dots \\ \phi^K \end{pmatrix} \quad \text{or} \quad \hat{A} \hat{V}_{los} = \hat{\phi}_{obs} \quad (4)$$

where \hat{A} is a new matrix with $3 \left(\sum_{k=1}^K N^k - 1 \right) \times \sum_{k=1}^K M^k$

dimension, \hat{V} is a new unknown velocity vector, and $\hat{\phi}_{obs}$ is a new observation vector. If only two ascending and descending SAR data, Eq. (4) can be further simplified, (Samsonov and d'Oreye, 2012).

Due to the inconsistency of acquisition dates of ascending and descending data, which results in rank deficiency of Eq. (4) and no unique solution. This problem can be solved under the least-square norm by applying SVD and the zero-, first-, or second-order Tikhonov regularization. Once the unknown velocity vector for each pixel are solved, the time series deformation can be obtained easily by integrating the deformation in each neighbouring SAR acquisition dates. It is worth noting that the integration cannot be executed directly due to the inconsistency of ascending and descending data acquisition dates. Therefore, it is necessary to take boundary correction for both ascending and descending SAR images to make the first and the last ascending and descending images are corresponding to the same dates, respectively.

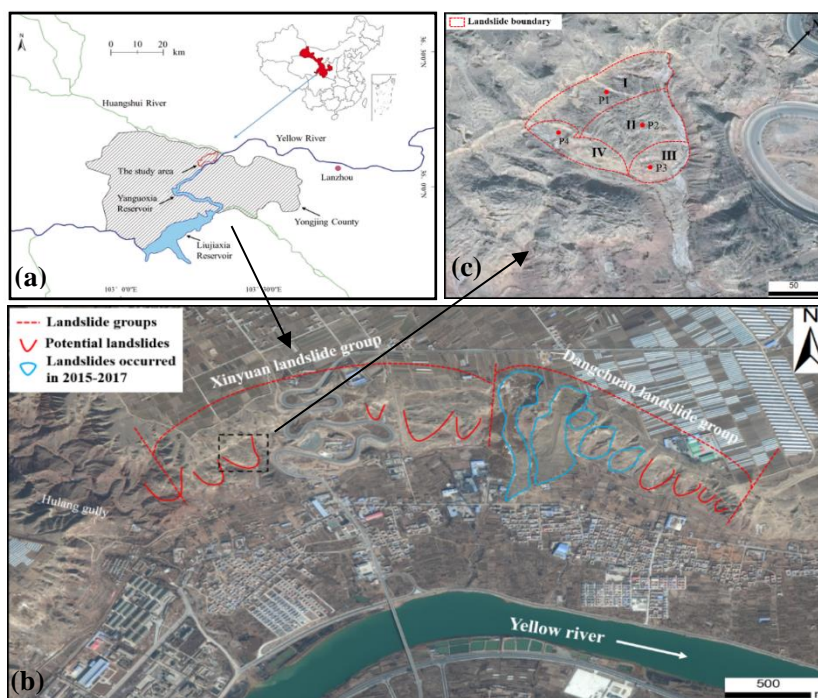


Figure 1. (a) Location of study region; (b) a wide view of the landslides in study area; (c) zoom in Xinyuan No.2 landslide, where points P1-P4 will be analyzed in Figure 4.

3. TEST AND RESULTS ANALYSIS

3.1 Test and results

In this test, twenty-three ascending and nineteen descending X-band Spot-mode TerraSAR-X data from January 2016 to

November 2017 are acquired to monitor the deformation of Xinyuan No.2 landslide. The data processing is divided into two steps. Firstly, differential interferograms of ascending and descending are generated independently, where 3m resolution unmanned aerial vehicle (UAV) DEM is applied to remove the

topographic phase. The temporal baseline and spatial baseline thresholds are set to 60 days and 250m, respectively. And multilooking number two is set in range and azimuth directions, respectively. The interferograms are filtered using the Goldstein filter method (Goldstein and Werner, 1998), unwrapped using minimum cost flow (MCF) algorithm. Followed by a combined model comprising a biquadratic model for orbital phase errors and a linear model for the elevation dependent errors including stratified atmospheric delay and topography errors (Kang et al., 2017). Finally, 32 ascending and 27 descending pairs of high quality interferograms are selected to calculate two-dimensional deformation rate and time series deformation results. To this end, all ascending and descending interferograms are geocoded and resampled to a common longitude and latitude grid of three

meters.

The one-dimensional LOS annual deformation rate maps for both ascending and descending data are shown in Figure 2. The maximum deformation rate of Xinyuan No.2 landslide in LOS of ascending and descending are about 60mm/year and -40mm/y, respectively. Then MSBAS technique is used to produce vertical and horizontal east-west annual deformation rate maps (Figure 3) and time series results. The two-dimensional time series of point P1-P4 in Figure 1(c) are shown in Figure 4. The results show that annual deformation rate of Xinyuan No.2 landslide in east-west and vertical directions reached -60mm and 30mm from 2016 to 2017, respectively.

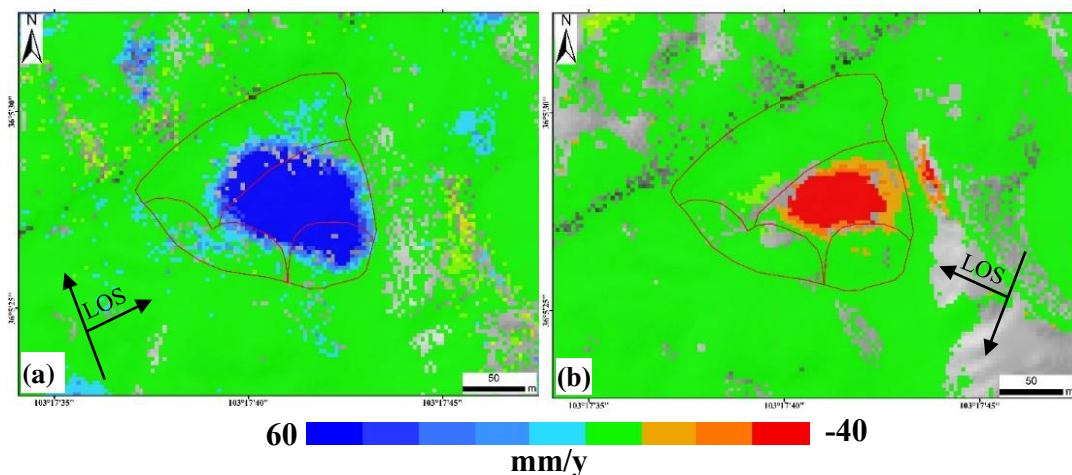


Figure 2. Annual deformation rates in line-of-sight direction calculated with SBAS technique. (a) ascending TerraSAR data and (b) descending TerraSAR data

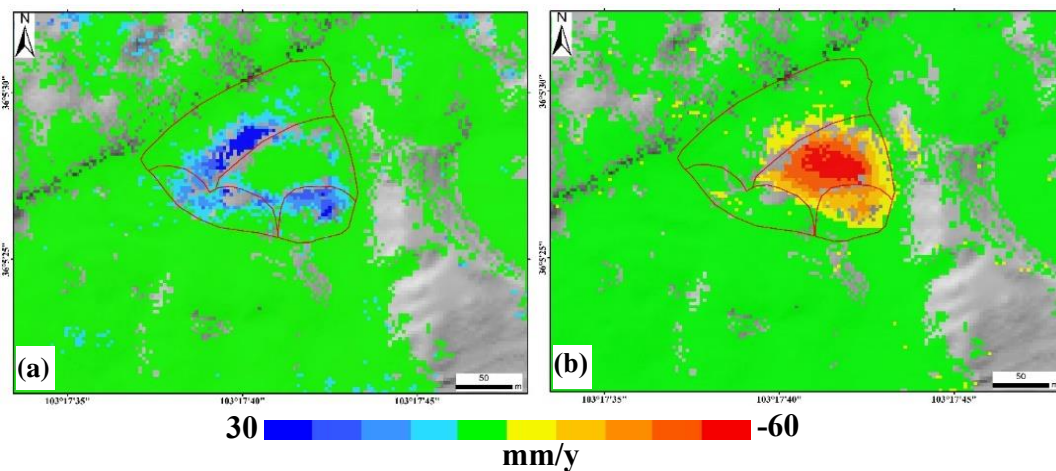


Figure 3. Annual deformation rates calculated with MSBAS technique. (a) in vertical direction and (b) in east-west direction

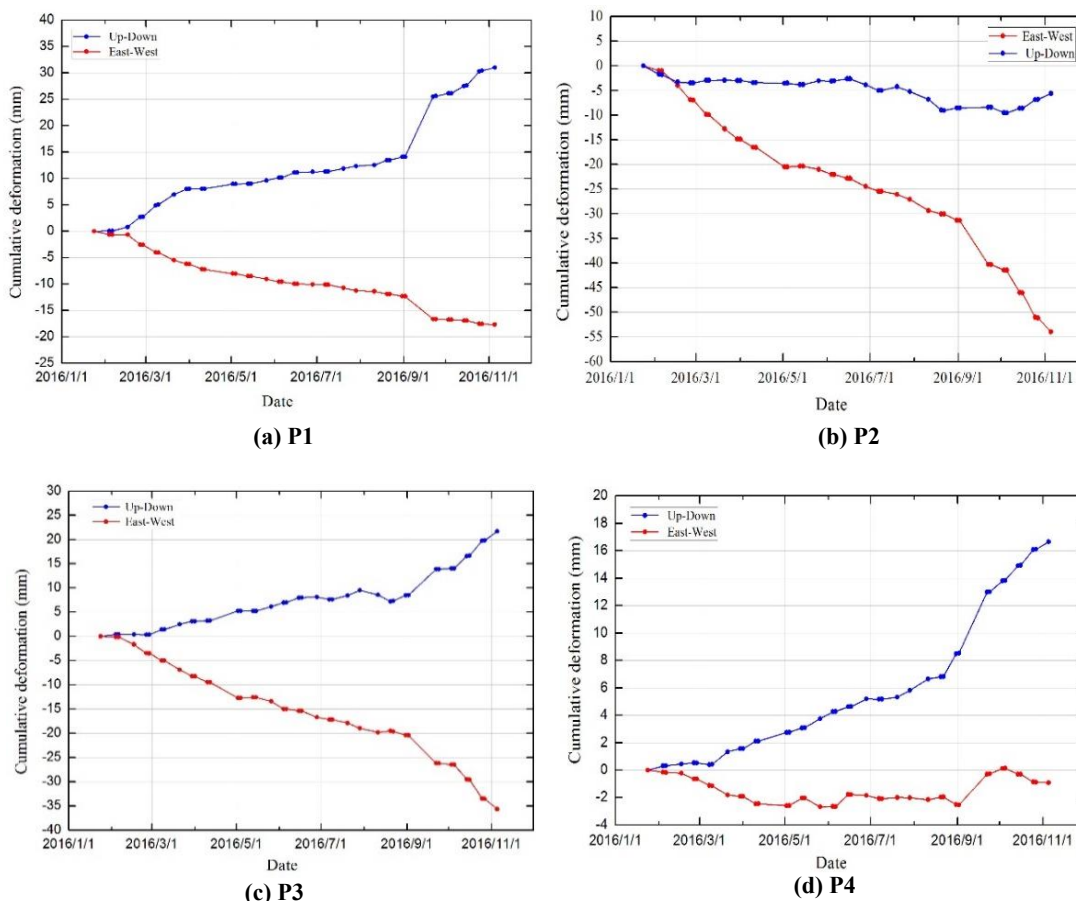


Figure 4. Time series deformation in vertical and east-west direction of Xinyuan No.2 landslide for points P1 to P4 shown in Figure 1(c) calculated with MSBAS technique.

3.2 Landslide mechanism analysis

It can be seen from Figure 3 that vertical deformation of this landslide is mainly occurred on the edge of the landslide (sections I, II, and III in Figure 1(c)), but horizontal deformation is obvious in the center of the landslide (section IV in Figure 1(c)). In Figure 4, two-dimensional time series deformation of four typical points from section I, II, III and IV in Figure 1(c) are shown, where vertical and east-west deformation is observed simultaneously at the points of P1 and P3, but vertical deformation is larger than east-west deformation at P1 and east-west deformation is larger than vertical deformation at P3. Besides, there is only east-west deformation at P2, and only vertical deformation at P4. The abovementioned phenomena are related to the retrogressive characteristic of the loess landslide shown in Figure 5 (Qi et al., 2017), including the following steps:

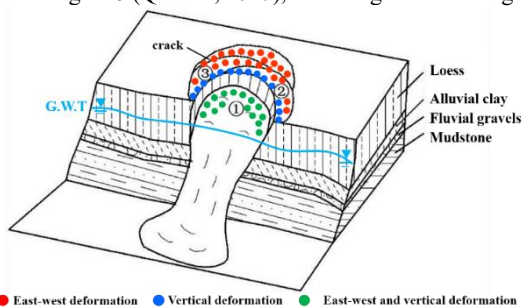


Figure 5. A conceptual model of the multi-staged retrogressive failure of loess landslide.

- 1) Groundwater level rising caused by the agricultural irrigation. Hence the basal zone of loess is softened by water saturation and prone to deformation under overburden stress, resulting in the first landslide ①;
- 2) Once a new free face is produced after the first landslide, the previous groundwater level increases, and the stress of the back edge for landslide continues to change, which caused nearly vertical cracks and forms the second landslide ②;
- 3) The failure procedure is repeated to form retrogressive landslide ③ etc.

4. CONCLUSIONS

In this study, the two-dimensional deformation rate maps and time series results in both vertical and east-west direction is introduced and tested for Xinyuan No.2 landslide. The retrogressive characteristic of loess landslide is revealed successfully by MSBAS technique, which indicates that the MSBAS method is a promising technique in landslide monitoring and mechanism analysis.

ACKNOWLEDGEMENTS

This research was funded by National Program on Key Basic Research Project (973 Program) (Grant No. 2014CB744703) and Natural Science Foundation of China projects (NSFC) (Grant No. 41731066 and 41628401). TerraSAR data are provided by DLR under grant GEO3039.

REFERENCES

- Berardino, P., Fornaro, G., Lanari, R., Sansosti, E., 2002. A new algorithm for surface deformation monitoring based on small baseline differential SAR interferograms. *IEEE Transactions on Geoscience and Remote Sensing*, 40(11), pp. 2375-2383.
- Goldstein, R., Werner, C., 1998. Radar interferogram filtering for geophysical applications. *Geophysical Research Letters*, 25(12), pp. 4035-4038.
- Kang, Y., Zhao, C. Y., Zhang, Q., Lu, Z., Li, B., 2017. Application of InSAR Techniques to an Analysis of the Guanling Landslide. *Remote Sensing*, 9 (10), pp. 1-17.
- Peng, D. L., Xu, Q., Liu, F. Z., He, Y. S., Zhang, S., Qi, X., Zhao, K. Y., 2017. Distribution and failure modes of the landslides in Heitai terrace, China. *Engineering geology*, pp. 1-15.
- Qi, X., Xu, Q., Liu, F. Z., 2017. Analysis of retrogress loess flowslides in Heifangtai, China. *Engineering Geology*, pp. 1-10.
- Rosi, A., Tofani, V., Tanteri, L., Stefanelli, C. T., Agostini, A., Catani, F., Casagli, N., 2017. The new landslide inventory of Tuscany (Italy) updated with PS-InSAR: geomorphological features and landslide distribution. *Landslides*, 1, pp. 1-15.
- Samsonov, S. V., d'Oreye, N., 2012. Multidimensional time-series analysis of ground deformation from multiple InSAR data sets applied to Virunga Volcanic Province. *Geophysical Journal International*, 191, pp. 1095-1108.
- Samsonov, S. V., d'Oreye, N., Smets, B., 2013. Ground deformation associated with post-mining active at the French-German border revealed by novel InSAR time series method. *International journal of applied earth observation and geoinformation*, 23, pp. 142-154.
- Samsonov, S. V., K. F. Tiampo, A. G. Camacho, Fernandez, J., Gonzalez, P. J., 2014. Spatiotemporal analysis and interpretation of 1993-2013 ground deformation at Campi Flegrei, Italy, observed by advanced DInSAR. *Geophys. Res. Lett.*, 41, pp. 6101-6108.
- Tiampo, K. F., Gonzalez, P. J., Samsonov, S. V., Fernandez, J., Camacho, A., 2017. Principal component analysis of MSBAS DInSAR time series from Campi Flegrei, Italy. *Journal of volcanology and geothermal research*, pp. 139-153.
- Xu, L., Dai, F. C., Tham, L.G., Tu, X. B., Jin, Y. L., 2011. Landslides in the transitional slopes between a Loess Platform and River Terrace, Northwest China. *Environ. Eng. Geosci.*, 17(3), pp. 267-279.
- Zhao, C.Y.; Kang, Y.; Zhang, Q.; Zhu, W.; Li, B. (2016): Landslide detection and monitoring with InSAR technique over upper reaches of Jinsha river, China: Geoscience and Remote Sensing Symposium. IEEE, pp. 2881-2884.
- Zhang, M. S., Li, T. L., 2011. Triggering factors and forming mechanism of Loess landslides. *Journal of Engineering Geology*, 19(4), pp. 530-540.
- Zhao, C.Y., Lu, Z., Zhang, Q., Fuente, J. D. L., 2012. Large-area landslide detection and monitoring with ALOS/PALSAR imagery data over Northern California and Southern Oregon, USA. *Remote sensing of Environment*, 124(9), pp. 348-359.
- Zhao, C. Y., Zhang, Q., He, Y., Peng, J. B., Yang, C. S., Kang, Y., 2016. Small-scale loess landslide monitoring with small baseline subsets interferometric synthetic aperture radar technique-case study of Xingyuan landslide, Shaanxi, China. *Journal of applied remote sensing*, 10(2), pp. 1-14.